

RECEIVED
 07 August 2018

REVISED
 17 August 2018

ACCEPTED FOR
 PUBLICATION
 7 September 2018

PUBLISHED
 12 September 2018

Structural, Electronic and Elastic Properties of rhombohedral phase $\text{Bi}_{0.5}\text{Na}_{0.5}\text{TiO}_3$ Using Density Functional Theory

M.H. Ridzwan^{1,4,*}, M.K. Yaakob^{1,4}, M.F.M. Taib^{1,4}, A.M.M. Ali^{1,4}, O.H. Hassan^{1,2}, M.Z.A. Yahya^{3,4}

¹Faculty of Applied Sciences, Universiti Teknologi MARA 40450 Shah Alam, Selangor, Malaysia

²Department of Industrial Ceramics, Faculty of Arts & Design, Universiti Teknologi MARA, 40450 Shah Alam, Malaysia

³Department of Defence Science, Universiti Pertahanan Nasional Malaysia, 57000 Kuala Lumpur, Malaysia

⁴Ionic Materials and Devices (iMADE) Research Laboratory, Institute of Science, Universiti Teknologi MARA, 40450, Shah Alam, Selangor, Malaysia

E-mail: mhaz_1110@hotmail.com

ABSTRACT: The structural, electronic and elastic properties of rhombohedral (R3c space group) $\text{Bi}_{0.5}\text{Na}_{0.5}\text{TiO}_3$ (BNT) were investigated via density functional theory (DFT) that implemented in the CASTEP computer code. The BNT properties were performed with local density approximation (LDA) and generalize gradient approximation (GGA). Calculated structural parameter and band gap are in good agreement with previous literatures. In calculated elastic constant, BNT shows higher resistant to compression stress compared to shear deformation. Also, the bulk modulus results show higher in value compared to the shear modulus, which imply that BNT is a hard and ductile material.

1. Introduction

In recent year, much effort on the modification of PZT has been done to enhance the piezoelectric properties through the addition of additives to replace either or both the A- or B-site ions [1]. However, usage of lead free piezoelectric ceramics is important as PZT contains hazardous lead toxicity [2]. Bismuth sodium titanate ($\text{Bi}_{0.5}\text{Na}_{0.5}\text{TiO}_3$ or BNT) would be an excellent candidate as a key toward lead free piezoelectric material that can replace PZT. BNT is a ferroelectric complex perovskite-structure compounds with two different ions at the A site of the ABO_3 structure. Moreover, BNT ceramic is strongly ferroelectric and have the Curie temperature $T_c = 320^\circ\text{C}$ [3], relatively with large remnant polarization $P_r = 38\mu\text{C}/\text{cm}^2$ [4], and coercive field $E_c = 73\text{kV}/\text{cm}$ [5] at room temperature. BNT with perovskite structure were used in many modern application such as non-volatile ferroelectric memory, dynamic random access memory, sensors and actuators [6].

As known, piezoelectric properties play a crucial role in any electrical material. This is due to its ability to generate electricity from pressure. Developments of this electrical property has brought innovations to actuators, sensors and ultrasonic transducers in the past [7]. One of the most famous and widely use piezoelectric material in the market is the lead zirconate titanate (PZT). Lead base piezoelectric has been use for years in many applications due to its superior dielectric, piezoelectric, and electromechanical coupling coefficients [7]. However, lead base material is also known for its toxicity in nature and degradations after number of cycles [8]. Eventually, the search of a new lead-free piezoelectric is currently in progress to produce a safe, eco-friendly piezoelectric. BNT could be a suitable material that can replace PZT, as it can reduce the usage of lead in the green technology devices [9].

In this study, the work focused on investigating the structural, electronic and elastic properties of BNT via quantum calculation using first principles calculation. First principle calculation has been proven to be an effectively predict and design a new ferroelectric materials that hard to established experimentally due to the difficulty to synthesis in conventional technique such as in dopant BNT [10,11], SnTiO_3 [12–14], GeTiO_3 [15] and also multiferroic materials [16–18]. Furthermore, there are very few theoretical studies on properties of BNT especially in elasticity of the material.

2. Experimental

2.1 Computational Method

First principles calculations of rhombohedral (R3c space group) BNT were performed using density functional theory (DFT) plane-wave pseudopotentials as implemented in Cambridge Serial Total Energy Package (CASTEP) computer code [19] within local density approximation (LDA) [20] and generalized gradient approximation (GGA) functionals [21]. The electrons orbital of Bi ($5d^{10}6s^26p^3$), Na ($3s^1$), Ti ($3d^2s^2$) and O ($2s^22p^4$) was treated as valence electrons. The geometry optimization was performed with convergence energy change per atom of below 5×10^{-6} eV, residual force less than 0.03 eV/\AA , stress threshold of below 0.05 GPa, and the displacement of atoms during geometrical optimization of less than 0.0005 \AA . A plane-wave cut off energy with 340 eV were applied. The Brillouin zone was optimized with $3 \times 3 \times 3$ k-point set via Monkhorst-Pack scheme for rhombohedral structure.

3. Results and discussion

The properties were first calculated by calculating the geometrical optimization of BNT. The optimized lattice parameter of BNT with rhombohedral (R3c space group) phase with its respective exchange correlation functional are presented in **Fig. 1** and compared in **Table 1**. The comparison study between the calculated result and experimental is carried out together with the calculation percentage different. From the calculation, it shows that LDA-CAPZ predicts the lattice parameter closer to experiments compared to other functionals. From this comparison, the results indicate that the functional LDA-CAPZ show the less differences among the calculated lattice parameters and provide the best agreement with the experimental result.

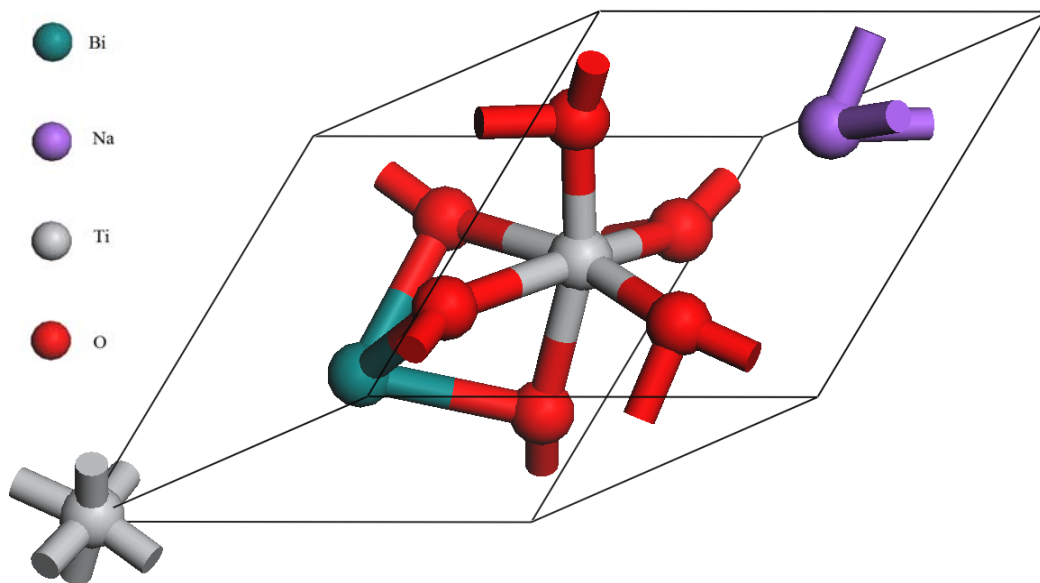


Figure 1: Crystal structure of BNT

Table 1: Calculated lattice constant, a, b, c (\AA) of rhombohedral structure (space group R3c) of BNT using different functional (LDA-CAPZ, GGA-PBE, and GGA-PBESol).

	LDA-CAPZ	GGA-PBE	GGA-PBESOL	Experiment [23]	Experiment [22]	Calculation [22]
Lattice parameter (\AA)	5.516	5.664	5.574	5.524	5.505	5.444
$a=b=c$						

The calculated electronic properties in this study is computed using the same exchange correlation approximation as mention above. **Table 2** show the result of calculated energy band from LDA-CA-PZ, GGA-PBE and GGA-PBEsol respectively.

Table 2: Calculated electronic band gap of BNT

Method	LDA	GGA-PBE	GGA-PBEsol	LDA [22]	GGA-PBE [23]	Experiment [24]
Energy Band Gap (eV)	2.813	2.560	2.694	2.820	2.100	~ 3.000

The band structure has energetically separate bands situated at different energy values. It is observed that the top of valence band (VB) and the bottom of conduction band (CB) are locate exactly at high symmetrical G point with direct band gap as shown in **Fig. 2** respectively. This shows that BNT has direct energy band gap. LDA that hold the shortest lattice parameter has the highest energy gap, 2.813 eV while GGA-PBE with the longest lattice parameter has lowest energy gap with 2.560 eV and GGA-PBESOL in between LDA and GGA-PBE has 2.694 eV. This trend shows that there is correlation between energy band gap and lattice parameter. **Table 2** above also compare present result to other theoretical study, and present result is good agreement with GGA method by Natanzon et al. and Min Zeng et al. [25,26] with 2 eV and 2.1 eV band gap energy.

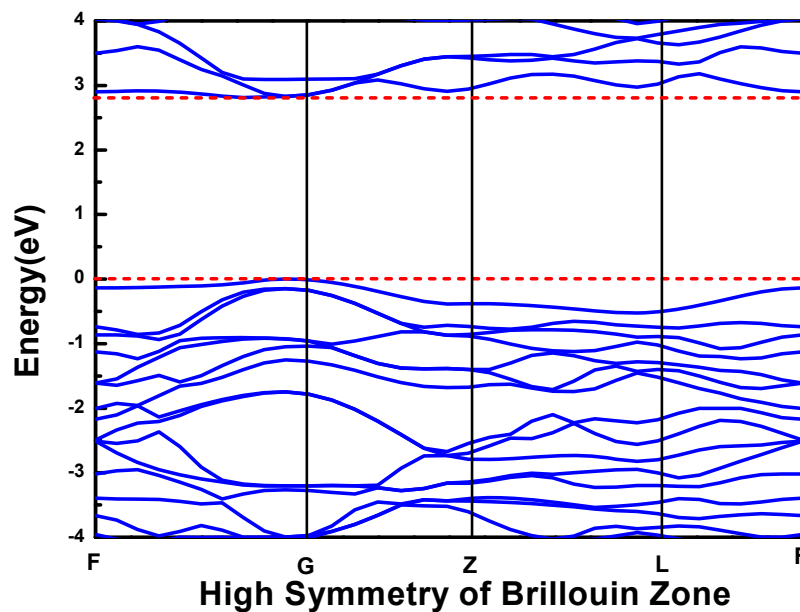


Figure 2: Electronic band structure BNT along the high symmetry axes of the Brillouin zone of functional LDA-CAPZ BNT

To further elucidate the nature of the electronic band structure, the total and atomic site partial densities of states (PDOS) of BNT has been calculated as shown in **Fig. 3**. From the density state, the main contribution of the valence band is the O-2p electrons, whereas the main contribution of conduction band are from Ti 3d and Bi 6p electrons. These bands show strong hybridization among them. This hybridization indicates the driving force of A and/or B-site driven ferroelectric materials [23]. Furthermore, a peak shown by Bi 6s in the valence band represent lone pair peak. This lone pair produces large ferroelectric polarization for this material [27]. This lone pair also contribute to the asymmetry charge distribution as shown in **Fig. 4**.

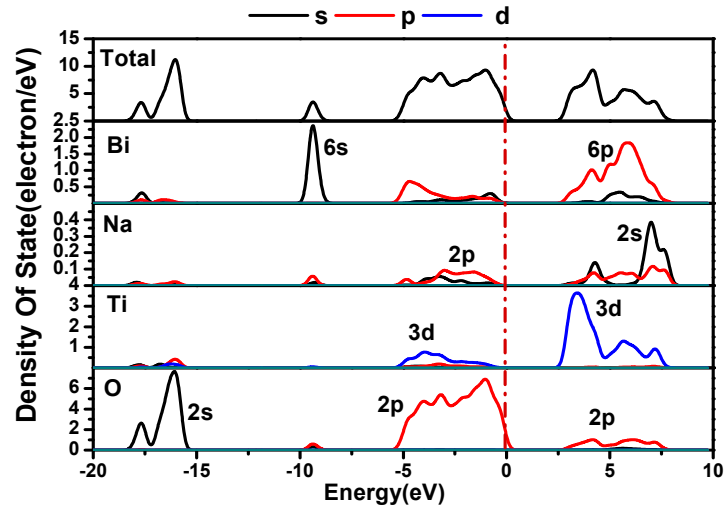


Figure 3: Partial Density of States (DOS) for LDA calculation BNT

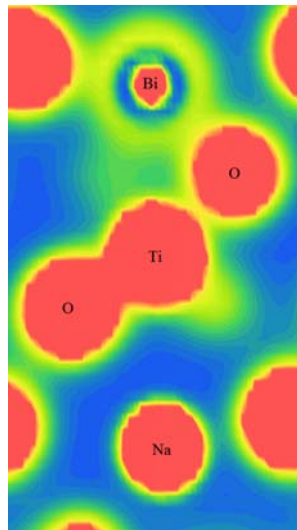


Figure 4: The chemical bonding of BNT.

Table 3: Elastic constant of BNT

	LDA	GGA-PBE	GGA-PBEsol	Experiment [4]	GGA [24]
C_{11}	256.6	214.7	264.9	153.9	368.8
C_{12}	101.8	80.9	99.4	18.7	120.3
C_{13}	77.8	46	79.5	52.1	141.1
C_{14}	4.6	16.6	12.3	-0.17	N/A
C_{33}	249.8	221.4	260.5	168.1	303.5
C_{44}	115.2	92.3	150.3	82.3	8.2
C_{66}	77.4	66.9	82.7	67.6	153.6

Elastic properties of solid are important to explain the mechanical behaviour and thermodynamic of material. From this work, we list six independent elastic stiffness tensors (C_{11} , C_{12} , C_{13} , C_{14} , C_{33} , C_{44} and C_{66}). From **Table 3** above it has been verified that all the calculation shows stable rhombohedral symmetry. Bulk modulus (B) and Shear modulus (G) can be calculated from this elastic constant by using Voigt-Reuss-Hill approximation. In general, GGA-PBE has lowest elastic constant and LDA has highest elastic constant. **Table 3** above also compared our calculated result with other study by Suchanicz et al. and Natanzon et al. [3,25]. Overall value show result of GGA-PBE calculation from this study closer to experimental result of Suchanicz et al. compared to other theoretical study. However, the different still significant.

Pugh [28] and Yaakob [27] describes that the bulk modulus represents the material resistance to fracture, whereas shear modulus represents the material resistance to elastic deformation. From the average elastic modulus value, the bulk modulus is higher than shear modulus, which indicates that BNT has higher compression stress resistant than shear resistant. Furthermore, the bulk and shear modulus shown in **Table 4**, relates to plastic deformation defined by Pugh [28] as the ratio of Hill's bulk modulus to Shear modulus, B_x/G_x . If $B_x/G_x > 1.75$, the material will behave like ductile. However, in this work, GGA-PBEsol of B_x/G_x is 1.49 which is less than 1.75. This shows that BNT is a hard material.

Table 4: Calculated bulk and shear modulus of BNT

	Bulk Modulus (GPa)			Shear Modulus (GPa)		
	B _V	B _R	B _H	G _V	G _R	G _H
LDA	141.97	95.27	139.68	94.32	183.33	208.026
GGA-PBE	129.51	82.16	128.02	80.14	128.77	81.15
GGA-PBEsol	145.23	96.92	144.07	95.65	144.65	96.29

4. Conclusions

The structural, electronic and elastic properties of BNT has been determined with first principles calculation with LDA-CAPZ, GGA-PBE and GGA-PBEsol functional. The functional LDA-CAPZ show the less different between calculated lattice parameter and provide the best agreement with the experimental result compared with GGA-PBE and GGA-PBEsol. The electronic band gap of rhombohedral (R3c) BNT are 2.813 eV, 2.560 eV and 2.694 eV using LDA-CAPZ, GGA-PBEsol and GGA-PBE, respectively. The partial density of states (PDOS) calculation show that the hybridization between O-2p at valence band and Ti-3d and Bi-6p at conduction band and Bi-6s in the valence band that represent lone pair peak. From calculated elastic constant, BNT has higher resistant to compression stress compare to shear deformation. We hope our studies pave ways for a better lead free BNT material.

Acknowledgement

This work was supported by the Fundamental Research Grant Scheme [Grant no. 600-IRMI/FRGS 5/3 (75/2016)] provided by the Ministry of Higher Education of Malaysia and Universiti Teknologi MARA (UiTM) Malaysia.

References

- [1] C.J. Walsh, W. A. Schulze, 14th IEEE Int. Symp. Appl. Ferroelectr. (2004) ISAF-04.
- [2] D. Damjanovic, N. Klein, J. Li, V. Porokhonsky, *Funct. Mater. Lett.* 03 (2010) 5–13.
- [3] J. Suchanicz, *J. Mater. Sci.* 37 (2002) 489–491.
- [4] J. Zhou, W.W. Peng, D. Zhang, X.Y. Yang, W. Chen, *Comput. Mater. Sci.* 44 (2008) 67–71.
- [5] H.B. Lee, D.J. Heo, R.A. Malik, C.H. Yoon, H.S. Han, J.S. Lee, *Ceram. Int.* 39 (2013) S705–S708.
- [6] A. Paul Blessington Selvadurai, V. Pazhivelu, B.K. Vasanth, C. Jagadeeshwaran, R. Murugaraj, *J. Mater. Sci. Mater. Electron.* (2015).
- [7] T.R. Shrout, S.J. Zhang, *J. Electroceramics.* 19 (2007) 111–124.
- [8] N.H. Hussin, M.F.M. Taib, O.H. Hassan, M.Z.A. Yahya, *Mater. Res. Express.* 4 (2017) 074001.
- [9] W.C. Lee, Y.F. Lee, M.H. Tseng, C.Y. Huang, Y.C. Wu, *J. Am. Ceram. Soc.* 92 (2009) 1069–1073.
- [10] A. Prado-Espinosa, J. Camargo, A. del Campo, F. Rubio-Marcos, M. Castro, L. Ramajo, *J. Alloys Compd.* 739 (2018) 799–805.
- [11] S. Hajra, S. Sahoo, M. De, P.K. Rout, H.S. Tewari, R.N.P. Choudhary, *J. Mater. Sci. Mater. Electron.* 29 (2018) 1463–1472.

- [12] M.F.M. Taib, M.K. Yaakob, A. Chandra, A.K. Arof, M.Z.A. Yahya, *Adv. Mater. Res.* 501 (2012) 342–346.
- [13] M.F.M. Taib, M.K. Yaakob, O.H. Hassan, A. Chandra, A.K. Arof, M.Z.A. Yahya, *Ceram. Int.* 39 (2013) 297–300.
- [14] N.H. Hussin, M.F.M. Taib, N.A. Johari, F.W. Badrudin, O.H. Hassan, M.Z.A. Yahya, *Appl. Mech. Mater.* (2014) 57–62.
- [15] M.F.M. Taib, M.K. Yaakob, M.S.A. Rasiman, F.W. Badrudin, O.H. Hassan, M.Z.A. Yahya, (2012) 708–712.
- [16] M.K. Yaakob, M.F.M. Taib, M.S.M. Deni, A. Chandra, L. Lu, M.Z.A. Yahya, *Ceram. Int.* 39 (2013) 283–286.
- [17] M.K. Yaakob, M.F.M. Taib, M.S.M. Deni, M.Z. a. Yahya, *Integr. Ferroelectr.* 155 (2014) 134–142.
- [18] M.K. Yaakob, M.F.M. Taib, O.H. Hassan, M.Z.A. Yahya, *Ceram. Int.* 41 (2015) 10940–10948.
- [19] S.J. Clark, M.C. Payne, *J. Phys.: Condens. Matter* 14 (2002) 2717–2744.
- [20] J.P. Perdew, A. Zunger, *Phys. Rev. B.* 23 (1981) 5048–5079.
- [21] Z. Wu, R. Cohen, *Phys. Rev. B.* 73 (2006) 235116.
- [22] H. Lü, S. Wang, X. Wang, *J. Appl. Phys.* 115 (2014) 0–7.
- [23] M. Zeng, S.W. Or, H.L.W. Chan, *J. Appl. Phys.* 107 (2010) 043513.
- [24] B. Andriyevsky, J. Suchanicz, C. Cobet, A. Patryn, N. Esser, B. Kosturek, *Phase Transitions.* 82 (2009) 567–575.
- [25] R. Bujakiewicz-Korońska, Y. Natanzon, *Phase Transitions.* 81 (2008) 1117–1124.
- [26] G. Wang, S. Wu, Z.H. Geng, S.Y. Wang, L.-Y. Chen, Y. Jia, *Opt. Commun.* 283 (2010) 4307–4309.
- [27] M.K. Yaakob, M.F.M. Taib, L. Lu, O.H. Hassan, M.Z.A. Yahya, *Mater. Res. Express.* 2 (2015) 116101.
- [28] S.F. Pugh, *Philos. Mag. Ser. 45* (1954) 823–843.

© 2018 by the authors. Published by EMS (www.electroactmater.com). This article is an open access article distributed under the terms and conditions of the Creative Commons Attribution license (<http://creativecommons.org/licenses/by/4.0/>).